Tracking urban resilience to disasters: a mobility network-based approach

Yan Wang
Charles E. Via, Jr. Department of Civil and Environmental Engineering, Virginia Tech
wangyan@vt.edu

John E. Taylor
School of Civil and Environmental Engineering, Georgia Tech
jet@gatech.edu

ABSTRACT

Disaster resilience is gaining increasing attention from both industry and academia, but difficulties in operationalizing the concept remain, especially in the urban context. Currently, there is scant literature on measuring both spatial and temporal aspects of resilience empirically. We propose a bio-inspired quantitative framework to track urban resilience to disasters. This framework was built upon a daily human mobility network, which was generated by geolocations from a Twitter Streaming API. System-wide metrics were computed over time (i.e. pre-, during and post-disasters). Fisher information was further adopted to detect the perturbation and dynamics in the system. Specifically, we applied the proposed approach in a flood case in the metropolis of São Paulo. The proposed approach is efficient in uncovering the dynamics in human movements and the underlying spatial structure. It adds to our understanding of the resilience process in urban disasters.

Keywords

Fisher information, human mobility, network analysis, Twitter, urban resilience

INTRODUCTION

Due to the increasing risk, frequency, and intensity of natural disasters caused by climate change, disaster resilience has gained momentum in both academic and policy discourse (Meerow, Newell, and Stults, 2016). Building urban resilience emerges as a critical agenda due to rapid urbanization, and extensive interconnected infrastructure systems in urban areas (Cutter et al., 2014). Resource dependencies of cities on surrounding or other areas can incur cascading impact on their dependent areas, and pre-existing urban stressors can aggravate the effects of climate change (Cutter et al., 2014). We lack a unified definition of disaster resilience. However, one that contains many characteristics of disaster resilience is from the National Academy of Sciences (NAS): "*the ability to prepare and plan for, absorb, recover from, and more successfully adapt to adverse events*" (Cutter et al., 2012). Resilience in the disasters research field, though overlapped with concepts of vulnerability and robustness, has a different emphasis on the dynamic process of adapting or recovering from natural disasters or extreme events (Hufschmidt, 2011; Zhou et al., 2010). Tailored to the urban context, disaster resilience should highlight both temporal and spatial scales. These scales can be used to describe its capability of maintaining or returning to desired functions, adapting to change, and transforming systems after perturbations (Meerow et al., 2016) to address the complexity and dynamics of cities.

Currently, it is still impossible to precisely predict the climate extremes in terms of spatial distribution and temporal evolution, regardless of their increased intensity or frequency (Linkov et al., 2014). These unknowns require redoubling operational efforts in building resilience. We need rigorous measurements to guide what and how to measure success (Garmestani et al., 2013; Spears et al., 2015). This is important because operationalizing the concept of urban resilience to disasters has been difficult to apply and manage; moreover, inappropriate usage of the term can bring significant negative impacts when guiding responses to natural disasters of urban systems (Angeler and Allen, 2016). However, the multiplicity and vague definitions of resilience increase difficulties to measure resilience. Cities, as complex systems, do not lend themselves easily to measurement. It is also difficult to access high-quality data during disasters to support quantification.

Fortunately, an array of approaches for assessments and quantitative measures of disaster resilience have been developed (Quinlan et al., 2015). Some conceptual frameworks have been proposed to quantify disaster resilience in a deterministic way for decision making in different scenarios, e.g., Zobel (2011), Zobel (2014), Zobel and

Khansa (2014), and MacKenzie and Zobel (2015). Most of them were based on the relationship between an initial impact of a disaster event and subsequent time to recovery. Some focused on empirical quantifications (Cimellaro et al., 2010; Pant et al., 2014; Cutter et al., 2014; Lam et al., 2015) from a specific perspective such as facility, economy, social, policy etc. Some of these studies have examined the dynamic nature of resilience over time, especially for the recovery process (e.g. Pant et al., 2014; Zobel, 2014). Few scholars have recognized the importance of spatial and temporal attributes of resilience. For example, Frazier et al. (2013) built a set of place-specific indicators to estimate baseline resilience at a community level. However, these studies cannot capture spatio-temporal dynamics of resilience over the course of a disaster in terms of urban structure involving human activities. We need to study the dynamics from this new perspective to understand the holistic process of perturbation and recovery of both urban spatial structure and human movements.

To address the methodological challenges, we investigated bio-inspired approaches in the research area of ecology, which is the original study field of resilience. As resilience has emerged as a unifying concept across various disciplines including ecology and disaster management (Quinlan et al., 2015), approaches to quantifying resilience in ecology can provide diverse and fundamental insights in tracking urban resilience to disasters. We identified two effective tools in assessing and measuring resilience in this field: *network analysis* and *Fisher information*.

Network analysis has been proven to be a useful quantitative tool for exploring social-ecology resilience and tracking changes in vulnerability (Moore et al., 2014; Moore et al., 2015). It represents the complex ecology system as an aggregation of vertices and edges and makes it possible to be analyzed in standard mathematical approaches. Moreover, network analysis can also describe the connectivity among fragmented landscapes (Estrada and Bodin, 2008), characterize the spatially structured population in these landscapes (Bodin and Norberg, 2007), and disentangle the complexity within the spatio-temporal interactions between individuals and their environment (Jacoby and Freeman, 2016). These advantages show its potential in capturing the dynamic process of urban systems involving both human movements and spatial structure during natural disasters.

Fisher information (FI) was developed by Ronald Fisher (1922) as a measure of the amount of information of a parameter from observable data. It has been effectively used in measuring resilience in ecological systems by assessing changes in variables that charaterize the condition of the system (Eason and Cabezas, 2012; Eason et al., 2016; Karunanithi et al., 2008; Spanbauer et al., 2014). This information theory-based approach is beneficial in detecting both swift and subtle changes in system dynamics (Eason et al., 2016). Cities affected by disasters, involving fragmented spatial structure and perturbed human movements, are characterized by complexity. The complementary perspectives of networks and information processing are effective in describing complex systems. Therefore, we propose to combine the two tools to track the process of disaster resilience in cities.

Recent developments in information technology have provided an unprecedented amount of spatio-temporal data from diverse sources to study urban issues, such as human mobility patterns (Yan et al., 2014), human diffusion and city influence (Lenormand et al., 2015), land use and mobility (Lee and Holme, 2015), congested travels (Çolak et al., 2016), spreading of infectious disease (Brockmann et al., 2009), dynamic urban spatial structure (Louail et al., 2015; Noulas et al., 2015), and disaster resilience (Wang and Taylor, 2014, 2016). We also take advantage of these large-scale geolocations to bridge the data gaps in measuring disaster resilience. To begin, we used the human mobility network to describe the dynamic urban system. The movement network is reliant on the underlying urban spatial structures and social environment; it can help to reveal the impact of extreme events on human movement, usage of urban space, and spatial structure. The network is formed from aggregated geolocations at a daily basis in a disaster-affected city. Then we adopt FI in evaluating changes in network metrics over time. This helps clarify the dynamic process of resilience from a temporal aspect. Our study uniquely combined the two tools to evaluate both spatial and temporal aspects of urban resilience in the research field of disaster management.

METHODS: A BIO-INSPIRED APPROACH

Defining Urban Resilience to Disasters for Measurement

Resilience, though adopted in physics to describe the ability of something to return to its original shape after external shocks, gained its currency in the research area of ecology with a variety of definitions and measurements (Davoudi et al., 2012). A useful definition defines resilience as "a measure of the persistence of systems and of their ability to absorb change and disturbance" Holling (1973, p.14) also proposed two distinct concepts of resilience: engineering resilience and ecological resilience. The former denotes the ability of a system bouncing back to an *equilibrium* to respond to shocks and perturbations, while the latter underscores an adaption of a system to an *alternative* or multiple stable status instead of a single-state equilibrium (Davoudi et al., 2012; Holling, 1986;

Holling, 1996). Further, Carpenter et al. (2001) extended the definition of ecological resilience to social-ecological resilience to address the ability of system to stay in the domain of attraction, to self-organize, and to adapt.

Although definitions of resilience vary among diverse applications in different backgrounds, these three definitions provide a shared theoretical foundation to quantify resilience. It also worth noting that the particular context of resilience and a distinct way to define it will largely determine how it is quantified (Quinlan et al., 2015). Therefore, it is important for us to define resilience before the quantification. In our research context, urban systems involving mobility and spatial structure are complex and intrinsically dynamic. As it is difficult to define the optimal state of urban systems and to measure the exact impact caused by disasters, it is inappropriate to assume that the system can bounce back to an equilibrium state after external perturbations. Additionally, it is also difficult to quantify the capability of a system in self-organization and adaptation to measure social-ecological resilience with current data. Therefore, we defined urban resilience to disasters to align with *ecological resilience* to incorporate the inherently dynamic nature of urban systems.

Construction of Human Mobility Network from Geo-enabled Tweets

The raw data for building our human mobility network is comprised of geotagged Tweets collected from Twitter Streaming API (Wang and Taylor, 2015). We used geotagging as the only filter to collect real-time Tweets. As 1.24% of Tweets are geotagged (Pavalanathan and Eisenstein, 2015) and the streaming API can collect 1% of Tweets, our database is representative in terms of geo-enabled Tweets. The Twitter geotags are based on GPS Standard Positioning Service which offers a worst-case pseudo-range accuracy of 7.8 meters with 95 percent confidence, and the positional accuracy is affected by weather and device factors (Swier et al., 2015). The data process map can be found in Figure 1. We filtered geolocations into a disaster-affected city, and aggregated the filtered data into a human mobility network on a daily basis. This choice of temporal scale for forming a network can measure changes in network metrics and detect nuanced changes of the daily mobility network over time. The human mobility network formed in this study is a *weighted undirected* network, where nodes are distinct geographical locations, edges are displacements between two locations, and the number of displacements between the same pair of locations is the weight of the edge regardless of the direction.

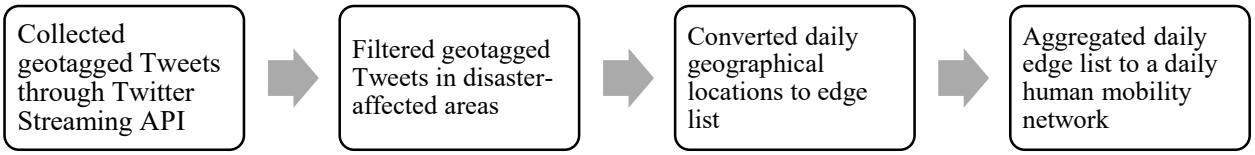

Figure 1. Process map of building Human Mobility Network

Network Metrics for Measuring Topological Dynamics

We considered a variety of network metrics to achieve a comprehensive description of a human mobility network (HMN) and the underlying urban spatial structure. One set of network metrics focus on *system-wide* properties, including number of vertices, number of edges, density, diameter, average path length, size of giant component, and global and local transitivity.

Specifically, *density* measures the proportion of displacements in HMN of all possible displacements in the same network. It can characterize the network-wide frequency of interactions between locations. *Diameter* of a mobility network is the maximal geodesic distance between any pair of locations, which reflects the ability of two locations to connect with each other. *Average path length* is the mean geodesic distance (ℓ) between two distinct locations in a network. *Giant component* describes all connected locations that a daily mobility network encompasses. *Transitivity* measures the probability that the adjacent locations of a trip are connected. We computed both *global transitivity* and *local average transitivity*. Global transitivity measures the fraction of triples that have their third edge filled in to complete the triangle. It is represented by the overall clustering coefficient $CI(g)$:

$$CI(g) = \frac{3 \times number\ of\ triangles\ in\ the\ network}{number\ of\ connected\ triples\ of\ nodes} \quad \text{(eqn. 1)}$$

where the connected triple refers to a node with edges to an unordered pair of nodes. While local transitivity is defined on an individual node basis:

$$CI_i(g) = \frac{number\ of\ triangles\ connected\ to\ location\ i}{number\ of\ triples\ centered\ at\ i} \quad \text{(eqn. 2)}$$

$$CI^{Avg}(g) = \frac{1}{n}\sum_{i} CI_i(g) \quad \text{(eqn. 3)}$$

Assortativity coefficient describes the level of homophily of a network (Newman, 2003). In HMN, this measurement quantifies the tendency of locations to be connected with other locations with similar connected displacements. We adopted the Pearson correlation coefficient with degree of adjacent vertices (Newman, 2002) (see eqn. 4 for the normalized correlation function).

$$r = \frac{1}{\sigma_q^2}\sum_{jk} jk\left(e_{jk} - q_j q_k\right) \quad \text{(eqn. 4)}$$

where q_k is the normalized distribution of remaining degree. σ_q^2 is the variance of q_k. e_{jk} is defined to be the joint probability distribution of the remaining degrees of the two vertices at either end of a randomly chosen edge. The coefficient lies between -1 to 1. Positive correlation indicates assortative mixing between locations of similar degree, while negative correlation is for disassortative mixing.

Fisher Information

We adopted FI to assess the process of perturbation and resilience in HMN. The form of FI in these studies are shown in equation eqn. 6 (Mayer et al., 2007).

$$FI = \int \frac{ds}{p(s)}[(dp(s))/ds]^2 \quad \text{(eqn. 5)}$$

Here, the urban mobility system is defined as a function of network variables which charaterize normal conditions and perturbed conditions due to extreme events. $p(s)$ refers to the probability of an observed network metric (s) of the urban system. The equation shows that FI is proportional to the change in the probability of observing an urban mobility state ($dp(s)$) versus the change in state (ds). In order to minimize the calculation errors, let $q^2(s) \equiv p(s)$,

$$FI = 4\int\left[\frac{dq}{ds}\right]^2 ds \quad \text{(eqn. 6)}$$

With discretization, $dq = q_i - q_{i+1}$ and $ds = s_i - s_{i+1}$. Additionally, the the state of the urban mobility system is denoted as ordinal number, $s_i - s_{i+1} = 1$. Therefore, the final equation for computing FI is:

$$FI = 4\int[q_i - q_{(i+1)}]^2 \quad \text{(eqn. 7)}$$

We interpreted the FI based on the *expanded Sustainable Regimes Hypothesis* (Karunanithi et al., 2008): (a) regimes are identified as periods with a stable and nonzero time-averaged FI; (b) a declining FI indicates a shift in a system with decreasing dynamic order; (c) an increasing FI signifies that the patterns are moving towards more stable patterns with increasing dynamic order; and (d) a regime shift is characterized by a steep drop in FI. Therefore, in this research, we assumed that the change of FI is consistent with dynamics of urban systems involving human movements and underlying spatial structures.

RESULTS

Overview of the Dataset

The metropolitan region of São Paulo, Brazil experienced a severe inland river flood during March 10 to 17, 2016 caused by extreme rainfall. São Paulo was selected as our studied area due to the high frequency of flooding in this area and its large urban population in South America (around 16 million inhabitants). This flood resulted in 24 casualties and 24 injured. The heavy rain began to fall on March 10, and ended the morning of March 11. 87.2 mm of rain was recorded in 24 hours in Mirante de Santana, north of São Paulo. We filtered collected geotagged Tweets into a *spatial bounding box* of the city of São Paulo with longitude from -47.3394 to -45.8134 and latitude from -24.1513 to -23.1762. The geographical box helps to include the largest size of flooding-affected area and population into our study. Five weeks of Tweets ranging from February 22 to March 27, 2016 are included in this study. This period consisted of two pre-flood and two post-flood weeks.

Pre-, During and Post-Flood Comparisons of Network-Wide Metrics

Over the five weeks, there are 2,449 daily average vertices (locations) and 2,194 daily average edges (displacements) included in a daily HMN. The dynamics of system-wide network metrics over weeks can be found in Figure 2. In this figure, each point represents a value of a network metric on a specific day. Each dashed line links the points to show the trend over time. Solid lines represent the Locally Weighted Scatterplot Smoothing of the scatter points. The two orange vertical lines define the duration of the flood event from March 10 to 17. The number of edges, number of vertices, and average degree (Figure 2(a-c)) follow a similar trend over time: all witness their peak values during the beginning four days of the flood event, and the values decrease with fluctuations after the peaks. The increased values at the beginning of the flood are likely to have been produced by the massive evacuation.

The value of edge density is very small (0.00068), which indicates that the daily aggregated mobility network is a sparse graph, and frequency of a displacement relative to another one is quite low in this network. The trend of this metric is quite steady and the impact of the flood is not obvious from visual inspection of the figure (Figure 2d).

Values of average path and network diameter also have similar trends over the weeks (Figure 2(e-f)). The mean geodesic distance between distinct pairs of locations achieves its highest value at 13.19 on March 10 when the flood began, then it drops to the lowest value of 5.83 on March 13. Similarly, on March 10, the diameter of the mobility network increases to 119. But four days later, HMN has the lowest diameter at 22. Both metrics keep increasing with fluctuations post-flood. These changes may have resulted from fragmentations in spatial structure and perturbations in the population's movements. The flooding led to a fragmented landscape, which further increased the geodesic distance between different locations; besides, due to the heavy rains and accumulation of water, the fragmentation increased, and most connections have been affected. Therefore, geodesic distances between locations decreased remarkably after its peak value during the flood event.

The more fragmented landscape and perturbed mobility can also decrease the transitivity of HMN (Figure 2(g-h)). Under the normal circumstances pre-flood, the daily average value of global transitivity was 0.65. This means that there is a high probability of two locations connected with each other when they are in adjacent trajectory. However, this average value decreases to 0.31 during the flood, and it is even lower (0.27) post-flood. Local average transitivity behaves similarly with average values of 0.36 (pre-flood), 0.16 (in-flood), and 0.20 (post-flood), respectively.

Interestingly, the relative size of the giant component (daily average 13.85%) during the disaster is larger than the size during normal days (daily average 8.41%) (Figure 2j). The number of vertices contributing to the giant component is different under the two circumstances: 360.38 under perturbed circumstances versus 205.18 under normal circumstances (Figure 2i). This can be caused by the reduction of displacements between affected areas and an increase of travels from affected areas to unaffected areas in the city.

The assortativity coefficient is highly responsive to the flood compared to other system-wide metrics (Figure 2k). The coefficients are negative pre- and post-flood, indicating a disassortative mixing of HMN: locations are not connected to locations with similar degree. However, during the most severe flooding period (from March 11 to 14), the coefficient becomes positive but small, which suggests that HMN exhibits a low degree of assortative mixing patterns: locations become more connected to locations with similar degree. This transition can also result from fragmented landscape and the evacuation, which make less affected area more connected with each other by people's movements, while more affected areas appear to have almost lost connections with other places.

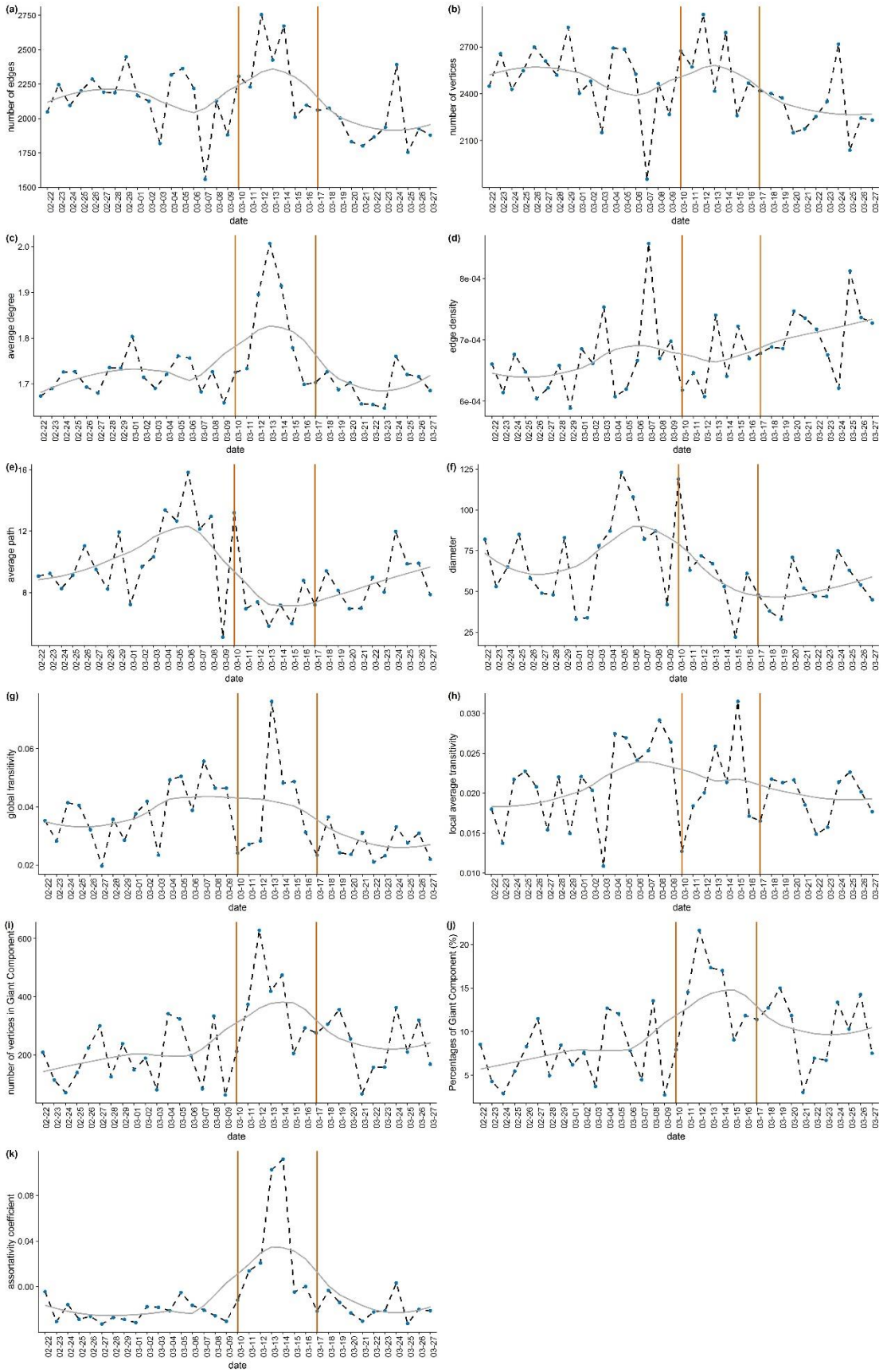

Figure 2. Dynamics of network-wide metrics over five weeks.

To further examine if the flood has statistically impacted the network-wide metrics, we conducted *adjacent-categories logistic regression* analysis to investigate the relationship between three states (i.e. pre-, during- and

post-disaster) and each distinct network metric. Adjacent category regressions are a specific form of generalized logistic regression for multinomial outcomes (O'Connell, 2006). This approach compares response outcomes of adjacent categories. Before the regression analysis, we performed the *runs test* (Bradley, 1968) for detecting the randomness in values of each network metric (Table 2). *p-values* of all data sets are larger than 0.05, which indicates that values of each network metric are random, and adjacent-categories logistic regression is appropriate to be used. We then set the three states as ordinal response variables (specifically, 0 for the pre-flood state, 1 for the state during the flood, 2 for the post-flood state), and set a network metric as an explanatory variable in each logit model. The outcomes and *p-values* can be found in Table 2.

For the comparisons between pre- and during-flood states, the significance tests of the logistic regression reveal that assortativity coefficient, average path, and size of giant component are three metrics that have been significantly impacted by the flood event ($p < 0.05$). In comparison, number of edges, vertices, average degree, and global transitivity only exhibit statistically significant differences post-flood. They are relatively resistant to the flood at the beginning. Notably, assortativity coefficient is the only metric that responds to each state change, but metrics such as edge density, diameter, and local transitivity are stable over the course of three adjacent periods.

Table 2. Randomness of values of network metrics and outcomes of adjacent-categories logistic regression and significance tests

	Standardized Runs Statistic	***p-value***	**pre vs. during**	***p-value***	**during vs. post**	***p-value***
number of edges	-1.884	0.05957	-0.003744	0.08848	0.008310	0.00573 **
number of vertices	0.34832	0.7276	-0.00192	0.3817	0.006196	0.0243 *
average degree	-1.1971	0.2313	-18.230	0.0514	35.072	0.0189 *
assortativity coefficient	- 0.85368	0.3933	-150.5485	0.00836 **	106.5233	0.04288 *
edge density	-0.85368	0.3933	-488.201	0.955	-14705.559	0.118
average path	-1.0449	0.296	0.5772	0.0305 *	-0.2863	0.2894
diameter	-1.5405	0.1234	0.01345	0.481	0.02629	0.282
global transitivity	-0.85368	0.3933	-0.7187	0.9836	137.7141	0.0337 *
local transitivity	-1.1971	0.2313	39.60258	0.670	41.15769	0.692
giant component (#)	-0.5103	0.6099	-0.0149	0.00875 **	0.00977	0.07024
giant componnet (%)	-2.0899	0.03663	-0.4375	0.0051 **	0.234	0.09743

Significance: '***' p<0.001; '**' p<0.01; '*' p<0.05.

Analysis of Resilience Based on Fisher Information (FI) of Network-Wide Metrics

We further computed the FI of all the network-wide metrics using a set of Python codes (Ahmad *et al.*, 2015). Each day was taken as a time step. Given the 35 days of data, eight time steps were set as a window size (Eason and Cabezas, 2012) to ensure that one point in the window does not improperly affect the general computation. The window increment was one time step. Herein, FI was integrated over an eight-day window that is moved forward in one-day increments. Values of a network metric in each time window were binned into discrete states. The probability density was then computed in each time window, and provided the basis for calculating FI. Figures 3 (a-k) are plots of FI for the 11 network-wide metrics over 28 days in the study. Metric values of the beginning eight days were used to calculate the initial value of FI. The orange bars highlight the flooding period and vertical grey lines define weeks.

According to the *expanded Sustainable Regimes Hypothesis* (Karunanithi et al., 2008), changes in values of FI can imply changes in regimes for the dynamic urban system. Except for FI of diameter, declining FI trends during the flooding period are found for almost all network metrics, indicating that the dynamic order decreases and the system becomes less stable. For network metrics—i.e. edge number (Figure 3a), vertice number (Figure 3b), average path (Figure 3f), and global transitivity (Figure 3h) —a local FI minimum occurs in the middle of the flooding period; for network metrics—i.e. average degree (Figure 3c), assortativity coefficient (Figure 3d), local transitivity (Figure 3i), and size of Giant Component (Figure 3k-j) —a local FI minimum occurs at the end of the flooding period. For all of these network metrics, their FI gradually increases after the lowest value, signalling the system gains dynamic order and becomes more stable. Post-flood values of FI may be lower or higher than the

pre-flood values, which indicates an alternative stable status rather than an equal stable status. For the overall system, results of the FI assessment of network-wide metrics indicate that the examined urban system exhibited no "regime shift" due to the flooding because there is no shifted FI value over the studied period. Additionally, the system exhibits resilience over the studied period: it lost dynamic order and became less stable during the flood, but gradually bounced back to an alternative stable status after the perturbation.

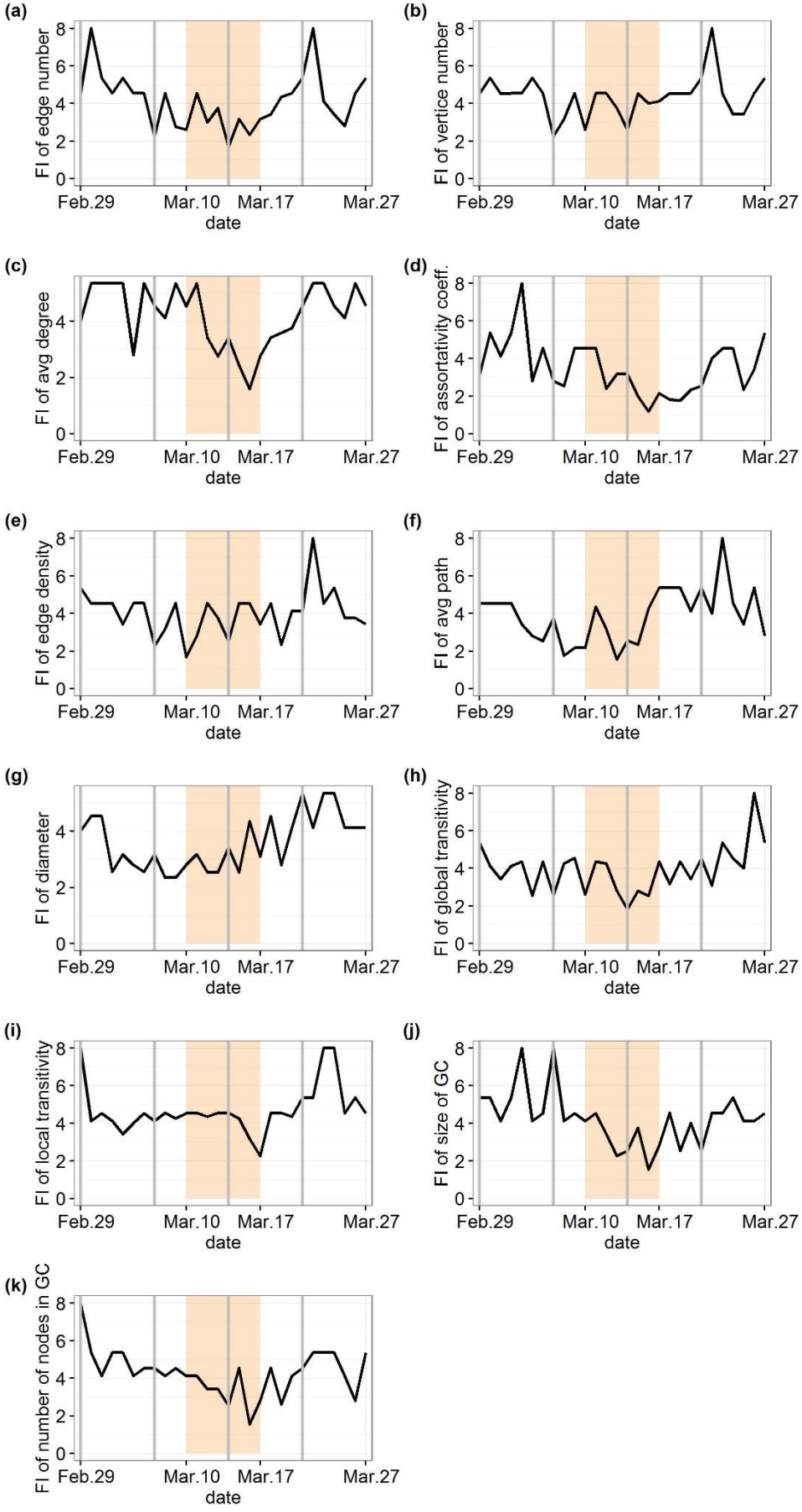

Figure 3. Trend of FI of network-wide metrics over time.

DISCUSSION

Previous work on measuring disaster resilience tends to be conceptual rather than quantitative (Cimellaro et al., 2010; Zobel, 2011; Zobel and Khansa, 2014). These resilience assessment frameworks have been applied to management systems and for building capacity in communities. Despite the fact that different dimensions of resilience have been addressed in different contexts and systems (Cutter et al., 2014; Cutter and Finch, 2008; Frazier et al., 2013; Lam et al., 2015), it is still difficult to quantify resilience in ways that are flexible and appropriate across a range of urban systems. Besides, although resilience has been identified as a dynamic process, few current assessments include the dynamics of how urban systems respond to disasters from both spatial and temporal aspects. Simultaneously, in spite of the shared theoretical foundations of resilience across different scientific disciplines, little cross-fertilization progress has been made, save for a handful of examples (Barrett and Constas, 2014; Quinlan et al., 2015). Our studies were inspired by definitions and approaches in measuring resilience in the pioneering field of resilience research: ecology. We applied network analysis in characterizing an urban system and used FI to detect dynamics in the resilience process.

Our constructed human mobility network can describe the dynamics of urban mobility and the underlying spatial structure. It is more representative of a general mobility network compared with networks formed from a single type of transportation mode. It is worth mentioning that our study is different from previous studies on modeling/simulating network resilience of infrastructure networks (e.g. freight transportation network, metro network, railway network, etc. (Miller-Hooks et al., 2012; Bhatia et al., 2015; Chopra et al., 2016; Gao et al., 2015; Wang, 2015)). Our research is focused on empirical data and used network metrics to describe the system. Our results show that most network metrics can capture the change of the urban mobility network and its underlying spatial structure. The *adjacent-categories logistic regression* further examined the statistically significant impacts of the flood. For distinct network metrics, the impact can be either at the beginning or at the end of the event. However, some network-wide metrics are less responsive to the perturbation of the flood. This indicates the intrinsic resilience of urban systems.

One limitation of our research is the sample size. Clearly, 2,449 daily average vertices in HMN are not enough to make generalizations about the network of all locations in a megacity. However, from the results, it can show the impact caused by the flood. With more geo-temporal data with higher resolution, a directed and weighted mobility network can be built to explore these concepts further. Additionally, a smaller time window (e.g. half day, hourly) and higher accuracy of geolocations can be used to form a network to achieve a more nuanced spatio-temporal analysis. Our proposed approach has only been applied in one type of natural disaster. With increasing availability of geographical and disaster data, this bio-inspired method can also be used in assessing urban resilience to other types of disasters such as hurricanes and earthquakes. And we can also compare resilience of the same type of disaster among distinct cities. In this way, we can explore the baseline of resilience and impact factors on the resilience, such as the scale of the study area, magnitude of disasters, etc. In terms of the research assumption, we used *ecological resilience* as the basis for quantification. With deeper understanding of urban systems, we may also assume urban resilience as socio-ecological resilience to explore and measure the capability of adaption and self-organization of systems.

CONCLUSIONS

Defining and measuring resilience is an important step to address challenges caused by natural disasters. It is of critical importance to help complex urban systems quickly recover and adapt when extreme events occur. Our study contributes to knowledge in the following ways. First, it adds to the paucity of empirical literature on measuring urban resilience to disasters. We provide a quantitative framework for describing and tracking the dynamic process of resilience in terms of human mobility and underlying spatial structure at both spatial and temporal scales. Second, our method is repeatable with large-scale crowed sourced spatio-temporal data from diverse resources such as mobile phone records, social media, GPS devices, etc. Upon further validation, it can be utilized at different scales (e.g. city, area, country and larger scales), and provide convenience for spatial comparisons. Third, it paves the way for further research on quantifying resilience of a larger complex system involving urban spatial structure and human movements; moreover, this study devotes effort in measuring resilience as a unifying concept across disciplines through a bio-inspired endeavor. In practice, combining with more detailed meteorological and geographical data, our framework can help disaster managers to trace and evaluate the process of perturbation and recovery more easily. This can further facilitate effective strategic decision making regarding when and where to arrange resources during and after disasters.

ACKNOWLEDGMENTS

This material is based upon work supported by the National Science Foundation under Grant No. 1142379 and the Virginia Tech BioBuild Interdisciplinary Graduate Education Program (IGEP). Any opinions, findings, and conclusions or recommendations expressed in this material are those of the authors and do not necessarily reflect the views of the National Science Foundation or the BioBuild program.

REFERENCES

Ahmad, N., Derrible, S., Eason, T., and Cabezas, H. (2015). Using Fisher Information in Big Data. arXiv preprint arXiv:1507.00389.

Angeler, D. G., and Allen, C. R. (2016). EDITORIAL: Quantifying resilience. Journal of Applied Ecology, 53(3), 617-624.

Barrett, C. B., and Constas, M. A. (2014). Toward a theory of resilience for international development applications. Proceedings of the National Academy of Sciences, 111(40), 14625-14630.

Bhatia, U., Kumar, D., Kodra, E., and Ganguly, A. R. (2015). Network science based quantification of resilience demonstrated on the Indian Railways Network. PLoS One, 10(11), e0141890.

Bodin, Ö., and Norberg, J. (2007). A network approach for analyzing spatially structured populations in fragmented landscape. Landscape Ecology, 22(1), 31-44.

Bradley, J. V. J. V. (1968). Distribution-free statistical tests.

Brockmann, D., David, V., and Gallardo, A. M. (2009). Human mobility and spatial disease dynamics. Reviews of Nonlinear Dynamics and Complexity, 2, 1-24.

Carpenter, S., Walker, B., Anderies, J. M., and Abel, N. (2001). From metaphor to measurement: resilience of what to what? Ecosystems, 4(8), 765-781.

Chopra, S. S., Dillon, T., Bilec, M. M., and Khanna, V. (2016). A network-based framework for assessing infrastructure resilience: a case study of the London metro system. Journal of The Royal Society Interface, 13(118), 20160113.

Cimellaro, G. P., Reinhorn, A. M., and Bruneau, M. (2010). Framework for analytical quantification of disaster resilience. Engineering Structures, 32(11), 3639-3649.

Çolak, S., Lima, A., and González, M. C. (2016). Understanding congested travel in urban areas. Nature Communications, 7.

Cutter, S. L., Ash, K. D., and Emrich, C. T. (2014). The geographies of community disaster resilience. Global Environmental Change, 29, 65-77.

Cutter, S. L., and Finch, C. (2008). Temporal and spatial changes in social vulnerability to natural hazards. Proceedings of the National Academy of Sciences, 105(7), 2301-2306.

Cutter, S. L., Joseph A. Ahearn, Bernard Amadei, Patrick Crawford, Elizabeth A. Eide, Gerald E. Galloway, and Goodchild, M. F. (2012). Disaster Resilience: A National Imperative. Washington, D.C.: National Academy of Sciences.

Cutter, S. L., W. Solecki, N. Bragado, J. Carmin, M. Fragkias, M. Ruth, and Wilbanks, a. T. J. (2014). Ch. 11: Urban Systems, Infrastructure, and Vulnerability. . Climate Change Impacts in the United States: The Third National Climate Assessment, 282-296. doi:doi:10.7930/J0F769GR

Davoudi, S., Shaw, K., Haider, L. J., Quinlan, A. E., Peterson, G. D., Wilkinson, C., . . . Davoudi, S. (2012). Resilience: A Bridging Concept or a Dead End?"Reframing" Resilience: Challenges for Planning Theory and Practice Interacting Traps: Resilience Assessment of a Pasture Management System in Northern Afghanistan Urban Resilience: What Does it Mean in Planning Practice? Resilience as a Useful Concept for Climate Change Adaptation? The Politics of Resilience for Planning: A Cautionary Note: Edited by Simin Davoudi and Libby Porter. Planning Theory and Practice, 13(2), 299-333.

Eason, T., and Cabezas, H. (2012). Evaluating the sustainability of a regional system using Fisher information in the San Luis Basin, Colorado. Journal of Environmental Management, 94(1), 41-49.

Eason, T., Garmestani, A. S., Stow, C. A., Rojo, C., Alvarez-Cobelas, M., and Cabezas, H. (2016). Managing for resilience: an information theory-based approach to assessing ecosystems. Journal of Applied Ecology.

Estrada, E., and Bodin, Ö. (2008). Using network centrality measures to manage landscape connectivity. Ecological Applications, 18(7), 1810-1825.

Fisher, R. A. (1922). On the mathematical foundations of theoretical statistics. Philosophical Transactions of the Royal Society of London. Series A, Containing Papers of a Mathematical or Physical Character, 222, 309-368.

Frazier, T. G., Thompson, C. M., Dezzani, R. J., and Butsick, D. (2013). Spatial and temporal quantification of resilience at the community scale. Applied Geography, 42, 95-107.

Gao, J., Liu, X., Li, D., and Havlin, S. (2015). Recent Progress on the Resilience of Complex Networks. Energies, 8(10), 12187-12210.

Garmestani, A. S., Allen, C. R., and Benson, M. H. (2013). Can law foster social-ecological resilience? Ecology and Society, 18, 37.

Holling, C. S. (1973). Resilience and stability of ecological systems. Annual Review of Ecology and Systematics, 1-23.

Holling, C. S. (1986). The resilience of terrestrial ecosystems: local surprise and global change. Sustainable Development of the Biosphere, 292-317.

Holling, C. S. (1996). Engineering resilience versus ecological resilience. Engineering within Ecological Constraints, 31, 32.

Hufschmidt, G. (2011). A comparative analysis of several vulnerability concepts. Natural Hazards, 58(2), 621-643.

Jacoby, D. M., and Freeman, R. (2016). Emerging network-based tools in movement ecology. Trends in Ecology and Evolution, 31(4), 301-314.

Karunanithi, A. T., Cabezas, H., Frieden, B. R., and Pawlowski, C. W. (2008). Detection and assessment of ecosystem regime shifts from Fisher information. Ecol Soc, 13(1), 22.

Lee, M., and Holme, P. (2015). Relating land use and human intra-city mobility. PLoS One, 10(10), e0140152.

Lenormand, M., Gonçalves, B., Tugores, A., and Ramasco, J. J. (2015). Human diffusion and city influence. Journal of The Royal Society Interface, 12(109), 20150473.

Linkov, I., Bridges, T., Creutzig, F., Decker, J., Fox-Lent, C., Kröger, W., . . . Nathwani, J. (2014). Changing the resilience paradigm. Nature Climate Change, 4(6), 407-409.

Louail, T., Lenormand, M., Picornell, M., Cantú, O. G., Herranz, R., Frias-Martinez, E., . . . Barthelemy, M. (2015). Uncovering the spatial structure of mobility networks. Nature Communications, 6.

Mayer, A. L., Pawlowski, C., Fath, B. D., and Cabezas, H. (2007). Applications of Fisher Information to the management of sustainable environmental systems Exploratory Data Analysis Using Fisher Information (pp. 217-244): Springer.

Meerow, S., Newell, J. P., and Stults, M. (2016). Defining urban resilience: A review. Landscape and Urban Planning, 147, 38-49.

Moore, C., Cumming, G. S., Slingsby, J., and Grewar, J. (2014). Tracking socioeconomic vulnerability using network analysis: insights from an avian influenza outbreak in an ostrich production network. PLoS One, 9(1), e86973.

Moore, C., Grewar, J., and Cumming, G. S. (2015). Quantifying network resilience: comparison before and after a major perturbation shows strengths and limitations of network metrics. Journal of Applied Ecology.

MacKenzie, C. A., & Zobel, C. W. (2015). Allocating Resources to Enhance Resilience, with Application to Superstorm Sandy and an Electric Utility. Risk Analysis.

Miller-Hooks, E., Zhang, X., & Faturechi, R. (2012). Measuring and maximizing resilience of freight transportation networks. Computers & Operations Research, 39(7), 1633-1643.

N. Lam, N. S., Reams, M., Li, K., Li, C., and Mata, L. P. (2015). Measuring community resilience to coastal hazards along the Northern Gulf of Mexico. Natural Hazards Review, 17(1), 04015013.

Newman, M. E. (2002). Assortative mixing in networks. Physical Review Letters, 89(20), 208701.

Newman, M. E. (2003). Mixing patterns in networks. Physical Review E, 67(2), 026126.

Noulas, A., Shaw, B., Lambiotte, R., and Mascolo, C. (2015). Topological properties and temporal dynamics of place networks in urban environments. Paper presented at the Proceedings of the 24th International Conference on World Wide Web.

O'Connell, A. A. (2006). Logistic regression models for ordinal response variables: Sage.

Pavalanathan, U., and Eisenstein, J. (2015). Confounds and consequences in geotagged Twitter data. arXiv preprint arXiv:1506.02275.

Pant, R., Barker, K., & Zobel, C. W. (2014). Static and dynamic metrics of economic resilience for interdependent infrastructure and industry sectors. Reliability Engineering & System Safety, 125, 92-102.

Quinlan, A. E., Berbés-Blázquez, M., Haider, L. J., and Peterson, G. D. (2015). Measuring and assessing resilience: broadening understanding through multiple disciplinary perspectives. Journal of Applied Ecology.

Spanbauer, T. L., Allen, C. R., Angeler, D. G., Eason, T., Fritz, S. C., Garmestani, A. S., . . . Stone, J. R. (2014). Prolonged instability prior to a regime shift. PLoS One, 9(10), e108936.

Spears, B. M., Ives, S. C., Angeler, D. G., Allen, C. R., Birk, S., Carvalho, L., . . . Pocock, M. J. (2015). FORUM: Effective management of ecological resilience–are we there yet? Journal of Applied Ecology, 52(5), 1311-1315.

Swier, N., Komarniczky, B., and Clapperton B. (2015). Using geolocated Twitter traces to infer residence and mobility. (GSS Methodology Series No 41). UK Retrieved from www.ons.gov.uk.

Wang, J. (2015). Resilience of Self-Organised and Top-Down Planned Cities—A Case Study on London and Beijing Street Networks. PLoS One, 10(12), e0141736.

Wang, Q., and Taylor, J. E. (2014). Quantifying human mobility perturbation and resilience in Hurricane Sandy. PLoS One, 9(11), e112608.

Wang, Q., and Taylor, J. E. (2015). Process Map for Urban-Human Mobility and Civil Infrastructure Data Collection Using Geosocial Networking Platforms. Journal of Computing in Civil Engineering, 04015004.

Wang, Q., and Taylor, J. E. (2016). Patterns and limitations of urban human mobility resilience under the influence of multiple types of natural disaster. PLoS One, 11(1), e0147299.

Yan, X.-Y., Zhao, C., Fan, Y., Di, Z., and Wang, W.-X. (2014). Universal predictability of mobility patterns in cities. Journal of The Royal Society Interface, 11(100), 20140834.

Zhou, H., Wan, J., and Jia, H. (2010). Resilience to natural hazards: a geographic perspective. Natural Hazards, 53(1), 21-41.

Zobel, C. W. (2011). Representing perceived tradeoffs in defining disaster resilience. Decision Support Systems, 50(2), 394-403.

Zobel, C. W. (2014). Quantitatively representing nonlinear disaster recovery. Decision Sciences, 45(6), 1053-1082.

Zobel, C. W., and Khansa, L. (2014). Characterizing multi-event disaster resilience. Computers and Operations Research, 42, 83-94.